

Formation and dissolution of D-N complexes in dilute nitrides

Marina Berti,* Gabriele Bisognin, Davide De Salvador, Enrico Napolitani, and Silvia Vangelista
MATIS CNR-INFM and Department of Physics, University of Padova, via Marzolo 8, 35131 Padova, Italy

Antonio Polimeni and Mario Capizzi
CNISM and Department of Physics, Sapienza Università di Roma, Piazzale A. Moro 2, 00185 Roma, Italy

Federico Boscherini
Department of Physics and CNISM, University of Bologna, Viale C. Berti Pichat 6/2, 40127 Bologna, Italy

Gianluca Ciatto
Synchrotron SOLEIL, L'Orme des Merisiers, Saint Aubin, Boîte Postale 48, F-91192 Gif sur Yvette Cedex, France

Silvia Rubini, Faustino Martelli, and Alfonso Franciosi
*Laboratorio Nazionale TASC INFM-CNR, Area Science Park, S.S. 14, Km. 163.5, 34012 Trieste, Italy
 and Center of Excellence for Nanostructured Materials, University of Trieste, 34127 Trieste, Italy*

(Received 3 August 2007; published 20 November 2007)

Deuterium (hydrogen) incorporation in dilute nitrides (e.g., GaAsN and GaPN) modifies dramatically the crystal's electronic and structural properties and represents a prominent example of defect engineering in semiconductors. However, the microscopic origin of D-related effects is still an experimentally unresolved issue. In this paper, we used nuclear reaction analyses and/or channeling, high resolution x-ray diffraction, photoluminescence, and x-ray absorption fine structure measurements to determine how the stoichiometric $[D]/[N]$ ratio and the local structure of the N-D complexes parallel the evolution of the GaAsN electronic and strain properties upon irradiation and controlled removal of D. The experimental results provide the following picture: (i) Upon deuteration, nitrogen-deuterium complexes form with $[D]/[N]=3$, leading to a neutralization of the N electronic effects in GaAs and to a strain reversal (from tensile to compressive) of the N-containing layer. (ii) A moderate annealing at 250 °C gives $[D]/[N]=2$ and removes the compressive strain, therefore the lattice parameter approaches that of the N-free alloy, whereas the N-induced electronic properties are still passivated. (iii) Finally, annealings at higher temperature (330 °C) dissolve the deuterium-nitrogen complexes, and consequently the electronic properties and the tensile strain of the as-grown GaAsN lattice are recovered. Therefore, we conclude that the complex responsible for N passivation contains two deuterium atoms per nitrogen atom, while strain reversal in deuterated GaAsN is due to a complex with a third, less tightly bound deuterium atom.

DOI: [10.1103/PhysRevB.76.205323](https://doi.org/10.1103/PhysRevB.76.205323)

PACS number(s): 71.55.Eq, 61.10.Nz, 61.85.+p, 61.72.Ji

I. INTRODUCTION

The incorporation of a few percent of nitrogen in GaAs or GaP leads to the formation of the so-called dilute nitrides. This particular type of material has attracted a lot of experimental and theoretical interest after the discovery that the introduction of nitrogen into the group V sublattice strongly affects the electronic, optical, and structural properties of the host matrix.^{1,2} In particular, the incorporation of a few percent of N atoms in GaAs leads to a substantial reduction in the band-gap energy³ and to a large distortion of the conduction band structure, with sizable changes in the transport,⁴⁻⁶ spin,⁷ and structural properties⁸ of the host crystal. Moreover, dilute nitrides are excellent candidates to overcome the current limits of the strain and band-gap engineering and to allow the design of a variety of devices such as high-efficiency hybrid solar cells and long wavelength lasers.²

It has been shown that all the effects associated with N in GaAs (and GaP) are dramatically affected by H irradiation, which restores in a controllable manner the pristine GaAs (and GaP) electronic properties (e.g., band-gap energy,⁹⁻¹¹ electron effective mass,^{12,13} and gyromagnetic factor⁷). Fur-

thermore, hydrogenation produces an astonishing reversal of the GaAsN lattice strain, from tensile to compressive.¹⁴⁻¹⁶ These H-related effects are particularly interesting since they provide an additional opportunity for defect and band-gap engineering in dilute nitrides.¹⁷

Therefore, a full comprehension of the microscopic mechanisms associated with N passivation in dilute nitrides is essential, and substantial efforts have been devoted in order to theoretically model the reaction between hydrogen and nitrogen in GaAsN and to account for all the experimental evidence.

To date, theoretical¹⁸⁻²⁰ and experimental^{21,22} studies indicate that a N-2H complex (formed by two H atoms bound to a single N atom), whose symmetry is distorted or canted from C_{2v} to C_{1h} , can explain most of the physical properties of hydrogenated dilute nitrides, except for the remarkable expansion of the lattice shown by high resolution x-ray diffraction (HRXRD) measurements in fully hydrogenated GaAsN.¹⁴⁻¹⁶ To this respect, it is important to notice that a moderate thermal annealing at 250 °C fully removes the lattice compressive strain but does not affect nitrogen passivation.¹⁵ This fact suggested that the hydrogenation-

induced compressive strain could be due to excess hydrogen atoms weakly bound to the N-2H structure. This picture has been supported recently by a theoretical study that indicates a N-4H complex (namely, *four* H atoms per N atom) as the final product of GaAsN hydrogenation.²³ This complex could account both for the compressive strain and for nitrogen passivation. Moreover, this complex could lose the *two* satellite H atoms and transform to the N-2H complex under mild annealing treatments, in qualitative agreement with experimental HRXRD results.¹⁵ Secondary ion mass spectrometry (SIMS) and photoluminescence (PL) measurements have also recently tried to pinpoint the exact [H]/[N] ratio in GaAsN/GaAs multiple quantum wells exposed to a H plasma for about 7 days.²⁴ Based on those measurements, it has been argued that up to *five* H atoms are bound to a single N atom and *at least three* H atoms are required to passivate N. However, it has been pointed out by the authors that this ratio may depend on the hydrogenation conditions, which in that case resulted in a severe sample etching. In conclusion, the number and type of N-H complexes responsible for nitrogen passivation and the value of the stoichiometric [H]/[N] ratio in these complexes are still debated and are important issues.

In the present work, we face these issues by combining selected nuclear reactions analyses (NRAs) and Rutherford backscattering spectrometry (RBS) with HRXRD, PL, and x-ray absorption near edge spectroscopy (XANES) measurements.

NRA concentration depth profiles show that D incorporation²⁵ initially proceeds in a “layer-by-layer” fashion leading to the formation of a N-3D complex, where *three* D atoms are bound to a single N atom. This complex induces both N electronic passivation and compressive strain. When the whole GaAsN layer has been passivated, D in excess is present in the samples. It is not bound to nitrogen and its concentration depth profile slightly extends into the GaAs substrate. The amount and the depth reached by this excess D are related to the hydrogenation conditions, which, on the contrary, do not affect the formation of the N-3D complexes.

The evolution of the N-3D complexes has been followed by investigating the deuterium concentration depth profiles, GaAsN lattice strain, and band-gap energy for different thermal annealing temperatures and times, up to the complete desorption of deuterium from the lattice. Upon a moderate annealing at 250 °C, the compressive strain vanishes, N is still electronically passivated, and the N-3D complexes convert into N-2D complexes. At temperatures equal to about 330 °C, the N-2D complexes dissociate, N passivation is lost, and the tensile strain is recovered. However, some excess deuterium, which is not bound to N, remains within the layers. Finally, at even higher temperatures (~600 °C), excess D atoms are fully removed from the sample and the hydrogen-free GaAsN lattice structure is completely recovered.

II. EXPERIMENT

GaAs_{1-x}N_x epilayers were grown by solid source molecular beam epitaxy on (001) GaAs substrates with an rf plasma

TABLE I. Sample name (first column) and thickness and composition (columns 2 and 3, respectively) measured by HRXRD rocking curves. Columns 4 and 5 report, respectively, the total nitrogen and deuterium doses for all the samples in which passivation of the whole layer was reached. N dose was determined from the ¹⁴N(*d*, α)¹²C reaction; D dose was determined from the ²H(*d*, *p*)³H reaction.

Sample	Thickness (nm)	N concentration (at. %)	d_N (10^{15} at./cm ²)	d_D (10^{15} at./cm ²)
E008	82±3	2.93±0.01	6.57±0.46	25.36±2.07
E271	280±10	1.27±0.01	7.85±0.47	28.31±2.31
E389	223±10	1.22±0.02	6.43±0.46	25.34±2.05
E510	110±5	1.40±0.02	3.23±0.45	13.00±1.18

source for N. Sample growth was performed at 500 °C after having grown a 500 nm thick GaAs buffer layer at 600 °C. Some samples had a few nanometers thick GaAs cap layer. Nitrogen was mixed in the plasma with argon and the rf source power used was in the 60–70 W range. In some cases, postgrowth thermal annealing at 660 °C for 60 min was used in order to improve the optical properties of the samples. The nitrogen concentration and thickness of the samples were determined by HRXRD (see Table I). Deuteration²⁵ was performed with a Kaufman source at 300 °C and D fluences d_D in the range 0.7×10^{18} – 5×10^{18} ions/cm² were employed in order to follow the evolution of the deuteration process up to full N passivation. The samples discussed in this paper were irradiated with an ion beam current density of 38 μA/cm². Deuterated samples were also produced by varying the current density from 7 to 65 μA/cm². The cooling procedure after deuteration was also varied.

Measurements of the lattice parameter were carried out using a Philips X’Pert PRO MRD diffractometer. The presence of a parabolic mirror and of an Anton Paar DHS 900 hot stage allowed us to collect high intensity (fast) and *in situ* (during annealing) diffraction measurements in a N₂ atmosphere. The x-ray wavelength was $\lambda_{\text{Cu K}\alpha_1} = 1.54056$ Å and the angular acceptance was 12 arc sec (triple axis configuration).

PL was excited with a neodymium-vanadate laser ($\lambda = 532$ nm) and spectrally analyzed by a single grating 0.75-m-long monochromator coupled to a cooled InGaAs linear array detector.

Following the procedure described in Ref. 8 and 26, a 1.2 D⁺ beam delivered by the CN accelerator at the Laboratori Nazionali di Legnaro (Italy) was used in order to perform RBS and nuclear reaction analysis with the ²H(*d*, *p*)³H and the ¹⁴N(*d*, α)¹²C reactions. Two silicon solid state detectors were connected to independent acquisition electronic systems in order to permit the simultaneous collection of NRA and RBS spectra both in random and in channeling conditions. NRA random spectra allowed getting the *total* nitrogen and deuterium doses, while [001] axial dips, simultaneously recorded on GaAs, nitrogen, and deuterium signals, allowed us to evaluate the alignment of the different elements to the matrix.

However, the D-induced reactions do not permit depth profiling. This is a strong limitation in the case of deuterium, whereas it is not important for nitrogen which has a constant concentration profile, as deduced by measuring constant depth-strain profiles in the as-grown samples. In order to obtain the deuterium concentration depth profiles, we used the less conventional ${}^3\text{He}(d,p){}^4\text{He}$ nuclear reaction.^{27–29} Since this reaction was never used before in the case of dilute nitrides, its feasibility has been carefully analyzed. After preliminary measurements in which the ion beam energy was varied in the interval 600–800 keV, the beam energy was set at 750 keV. This choice allows us to get the maximum of the cross section value at a depth into the samples corresponding to the GaAsN-GaAs substrate interface, while the cross section in the surface region was reduced by less than 8%.

The ${}^3\text{He}$ beam was delivered by the AN2000 accelerator at the Laboratori Nazionali di Legnaro (Italy). Also in this case, two independent acquisition systems allowed us to record contemporarily both RBS and NRA signals. The RBS detector was mounted in IBM³⁰ geometry at 150° , while a $1500\ \mu\text{m}$ surface barrier detector was mounted in Cornell geometry at the same scattering angle to detect the 13 MeV protons produced by the reaction. A circular tantalum diaphragm (4.0 mm diameter, 0.5 mm thick) was placed in front of the detector, together with a $10\text{-}\mu\text{m}$ -thick MylarTM foil, in order to stop all the spurious particles. NRA spectra were collected with both normal and 60° tilt angle incidences, the latter enhancing depth resolution by a factor of 2. Deuterium depth profiles were obtained by analyzing the spectra with the SIMNRA program.³¹ In any case, it was verified that the deuterium integral derived from the concentration depth profile was consistent (within the error bars) with the corresponding dose measured with the ${}^2\text{H}(d,p){}^3\text{H}$ reaction. This constraint, applied to the simulation procedure, allowed us to reach a best depth resolution of 50 nm.

N *K*-edge XANES measurements were performed at the ELETTRA synchrotron radiation facility in Trieste on the ALOISA undulator beamline.³² The photon flux on the sample was of the order of 5×10^{11} photons/s in a focal spot of $0.2 \times 0.5\ \text{mm}^2$; the value of the undulator gap was synchronized with the photon energy selected by the monochromator. Fluorescence detection was used in order to guarantee bulk sensitivity. The setup is based on the use of a windowless hyperpure Ge detector with a detection area of $\sim 100\ \text{mm}^2$ placed in the horizontal plane at 90° to the impinging photon beam at a distance of ~ 5 mm from the sample. The high brilliance photon beam coupled to the highly efficient detection scheme is mandatory in order to record good signal-to-noise ratio spectra from dilute elements in the soft x-ray range. A test measurement performed on a N-free sample (not shown) demonstrated that the N contamination on the surface is definitely negligible with respect to the signal originating from the bulk.

III. RESULTS

A. Complex formation

We have already shown¹⁵ that, independent of the growth technique (molecular beam or metallic-organic vapor phase

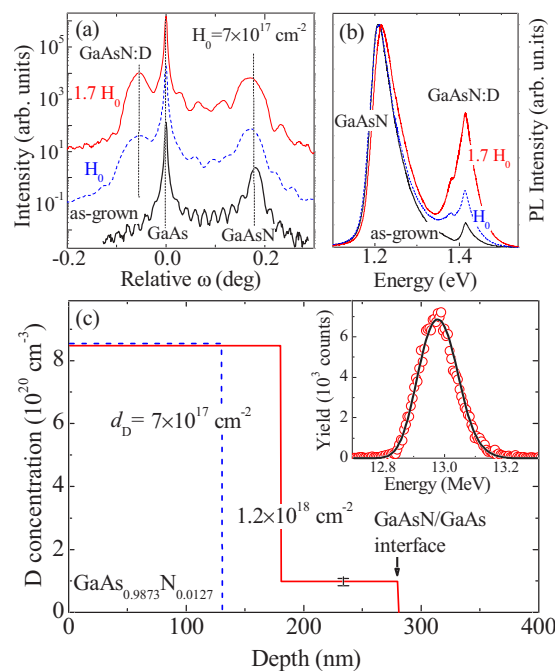


FIG. 1. (Color online) (a) (004) x-ray diffraction rocking curves of a 280-nm-thick $\text{GaAs}_{0.9873}\text{N}_{0.0127}$ sample before (bottommost curve) and after deuterium irradiation with doses $d_D = 7 \times 10^{17}$ and $1.2 \times 10^{18}\ \text{cm}^{-2}$ (middle and topmost curves, respectively). (b) Peak normalized photoluminescence spectra at $T=290\ \text{K}$ of the same samples displayed in (a). The same laser power density was used for all samples. (c) Deuterium depth profiles derived from NRA using the ${}^3\text{He}(d,p){}^4\text{He}$ reaction in the sample after different D irradiation fluences. Zero on the abscissa axis indicates the sample surface. The experimental spectrum of the $1.2 \times 10^{18}\ \text{cm}^{-2}$ irradiated sample, with its best simulation, is shown in the inset.

epitaxy) and of the N host lattice (GaAs or GaP), the hydrogen- or deuterium-induced compressive strain in fully hydrogenated and/or deuterated samples depends linearly on nitrogen concentration. Here, the evolution of the hydrogenation process has been investigated by measuring the HRXRD rocking curves (RCs) of samples irradiated with increasing deuterium fluences. These curves are shown in Fig. 1(a) for a 280-nm-thick $\text{GaAs}_{0.9873}\text{N}_{0.0127}$ sample (E271), as-grown and irradiated with d_D equal to 0.7×10^{18} and $1.2 \times 10^{18}\ \text{cm}^{-2}$. From the RC simulations, one finds that the thickness of the deuterium containing layers is equal to 130 ± 10 and 160 ± 20 nm for the lower and higher d_D values, respectively. PL measurements in these same samples show that the GaAs peak (corresponding to the N passivated layer) gains relative intensity with increasing d_D , consistently with RC results, see Fig. 1(b). The ${}^{14}\text{N}(d,\alpha){}^{12}\text{C}$ and ${}^2\text{H}(d,p){}^3\text{H}$ nuclear reactions²⁶ allowed us to get the total nitrogen and deuterium doses, while the corresponding D depth profiles, as measured by the ${}^2\text{H}({}^3\text{He},p){}^4\text{He}$ reaction, are shown in Fig. 1(c). Notice the good agreement between the thickness of the deuterated layers derived from HRXRD data in Fig. 1(b) and those found by NRA depth profiles displayed in Fig. 1(c). The inset shows the experimental spectrum with its simulation for the sample irradiated with $d_D = 1.2 \times 10^{18}\ \text{cm}^{-2}$. To get a further confirmation of the thickness

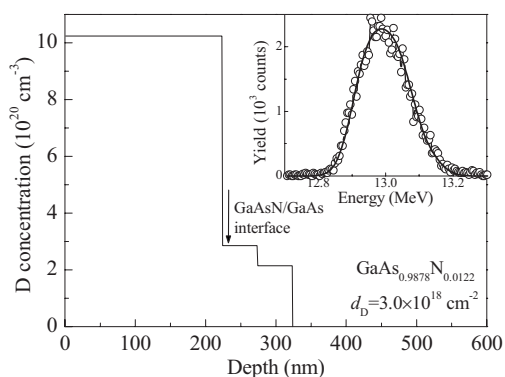


FIG. 2. Deuterium depth profile of a 223-nm-thick $\text{GaAs}_{0.9878}\text{N}_{0.0122}$ ($d_D = 3.0 \times 10^{18} \text{ cm}^{-2}$) as derived from NRA using the ${}^3\text{He}(d,p){}^4\text{He}$ reaction. Zero on the abscissa axis indicates the sample surface. The experimental spectrum with its best simulation is shown in the inset.

and the shape of concentration profiles derived from NRA, these samples were also measured with SIMS finding a very good consistency between the two techniques. SIMS was not used further due to the difficulty of getting good standards for the concentration and to avoid possible matrix effects.

Deuterium incorporation proceeds with a sharp front and a constant concentration into the reacted layer. From the nitrogen ($2.82 \times 10^{20} \text{ cm}^{-3}$) and deuterium ($8.52 \times 10^{20} \text{ cm}^{-3}$) concentrations measured in the D-containing part of the samples, one obtains that *there are three D atoms per N atom*, within experimental error, for both d_D values.

In order to get full passivation of the layers, most of the samples were deuterated with higher D fluences [$(3-5) \times 10^{18}$ ions/ cm^2]. Table I gives the total nitrogen and deuterium doses for all the samples in which passivation of the whole layer was reached. The corresponding GaAsN layer thickness and nitrogen concentrations are also reported. By looking at the data in Table I, it appears that in all the samples, the $[\text{D}]/[\text{N}]$ ratio reaches a value which is consistently higher than 3, in disagreement with the findings on partially reacted samples. However, it has to be pointed out that the values reported here come from NRA measurements performed with the deuteron-induced reactions, which only give the integral doses, disregarding the shape of concentration profiles.

The explanation of this discrepancy is provided by looking at D concentration depth profiles, as shown in Fig. 2 for sample E389 having N concentration equal to 1.22% (see Table I). The corresponding NRA spectrum and its simulation are shown in the inset. The concentration profile which gives the best simulation has a constant value up to a depth corresponding to the layer/buffer interface. However, a tail with a low concentration value extending into the GaAs buffer is necessary to get the best simulation of the experimental profiles. This deuterium in excess, which is obviously not bound to nitrogen, was never evidenced before. We always observed it in all the fully deuterated samples, and the parameters which govern its shape and the depth of its extension into the buffer are not completely clear at present. Nevertheless, it is clear that it influences the $[\text{D}]/[\text{N}]$ ratio

values, and its presence requires extreme care in determining the stoichiometry of the N-D complexes. A way to get a confirmation of the number of deuterium atoms bound to nitrogen in fully reacted samples is to consider a $[\text{D}]/[\text{N}]$ ratio interval whose limits are set by the ratio computed by considering all the deuterium in the GaAsN layer or the same deuterium amount after subtraction of a constant value corresponding to that of the maximum concentration in the excess tail. This is a rather rough procedure, and the $[\text{D}]/[\text{N}]$ ratios obtained have values ranging from 3.5 to 2.5 for all the samples.

In summary, on the basis of the whole set of results obtained both in fully and in not fully passivated samples where the extra D contribution is smaller, if any, we can conclude that the complex giving rise to *both* compressive strain and nitrogen passivation has three hydrogen atoms per single nitrogen atom.

B. Complex dissolution

We now address the issue of how many D (H) atoms are required to passivate a single nitrogen atom. It has been already shown that the compressive strain disappears upon a moderate annealing while nitrogen atoms remain passivated.¹⁵ This could be due either to a redistribution of the three D atoms in the N-3D complex or to the diffusion of one (or more) D atoms away from the N atoms. In order to distinguish between these two scenarios, the variations in the $[\text{D}]/[\text{N}]$ ratio as determined by NRA measurements have been correlated with the changes evidenced by diffraction measurements in deuterated samples submitted to different thermal annealings.

Figure 3(a) shows the evolution of the HRXRD rocking curves for different annealing stages as obtained in the same fully hydrogenated $\text{GaAs}_{0.9878}\text{N}_{0.0122}$ epilayer shown in Fig. 2.

By increasing the annealing time at a fixed temperature of 250 °C, the strain in the layer decreases with a monotonic trend, and after ~ 13 h, its value in the GaAsN layer is about null, i.e., the lattice parameter of N-free GaAs is almost achieved. However, PL measurements performed on this and similar samples at the end of the 250 °C annealing process show that nitrogen atoms are still fully passivated.¹⁵ A second transition from unstrained to a tensile strain has been observed in this same GaAsN layer by raising further the temperature, as shown in Fig. 3(b). After 20 min at 328 °C, the strain in the epilayer starts becoming tensile. After 280 min of annealing, the lattice parameter of pristine GaAsN is almost completely recovered as well as the band-gap energy the sample had before D irradiation, as found by PL measurements (not shown here). A full recovery of the initial tensile strain is obtained, however, only after an annealing at even higher temperatures (~ 600 °C). The evolution of the strain shown in Fig. 3, on one hand, confirms that the deuteration process is completely reversible and, on the other hand, indicates the existence of at least two different dissolution stages of the N-D complexes, which form right after D incorporation. Moreover, it shows that D removal occurs rather uniformly over the whole GaAsN layer, in con-

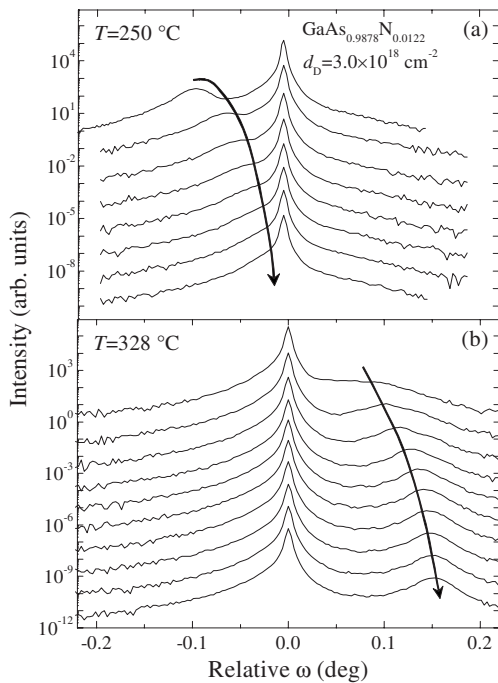


FIG. 3. (004) x-ray diffraction rocking curves of the same sample shown in Fig. 2 after sequential postgrowth treatments as indicated in the figure: (a) $T=250\text{ }^{\circ}\text{C}$ and (b) $T=328\text{ }^{\circ}\text{C}$. Annealing step intervals are equal to 120 and 30 min for (a) and (b), respectively.

trast with D incorporation that features a steplike behavior, see Fig. 1(c). These conclusions are supported by the deuterium concentration profiles in the GaAsN epilayer (sample E389) measured by NRA after the two annealing stages at 250 and 328 $^{\circ}\text{C}$ shown in Fig. 4. After annealing at the lower temperature, the deuterium concentration lowers uniformly within the whole GaAsN layer, where its value is constant. The excess deuterium tail, already present in the as-

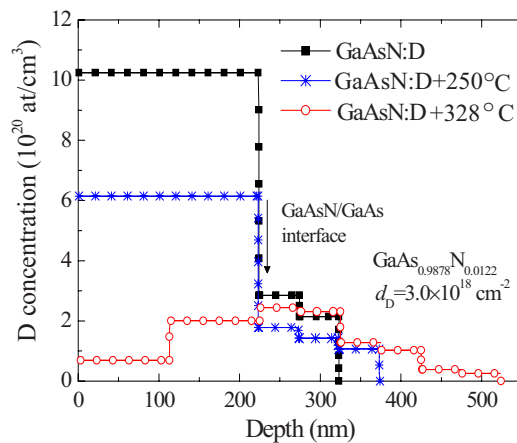


FIG. 4. (Color online) Deuterium depth profiles derived from the $^3\text{He}(d,p)^4\text{He}$ reaction in a 223-nm-thick $\text{GaAs}_{0.9878}\text{N}_{0.0122}$ sample at the end of the deuteration process (line+full squares), at the end of the 250 $^{\circ}\text{C}$ annealing stage (line+stars), and at the end of the 328 $^{\circ}\text{C}$ annealing stage (line+open circles). Zero on the abscissa axis indicates the sample surface.

deuterated sample, slightly broadens. After annealing at the higher temperature, the D concentration profile in the GaAsN layer decreases further: only a low concentration of excess D, quite broadened and peaked at the GaAsN/GaAs interface, is measured. After subtraction of the excess D measured beneath the GaAsN/GaAs interface, the difference in the $[\text{D}]/[\text{N}]$ ratio determined before and after annealing at 250 $^{\circ}\text{C}$ (no compressive strain, full N passivation) is equal to

$$\begin{aligned} [\text{D}]/[\text{N}]_{\text{as-deut}} - [\text{D}]/[\text{N}]_{\text{ann } 250\text{ }^{\circ}\text{C}} &= 7.6 \times 10^{20}/2.7 \times 10^{20} \\ &- 4.7 \times 10^{20}/2.7 \times 10^{20} = 1.1. \end{aligned}$$

This shows that the compressive strain is produced by the complex responsible for N passivation plus an additional, weakly bound satellite D atom, which is released already by the moderate energy supplied during the 250 $^{\circ}\text{C}$ annealing. Two D atoms remain, instead, bound to a single N atom in a N-2D complex, which passivates N and establishes a good lattice match to the GaAs substrate. This result agrees well with previous suggestions based on infrared absorption²¹ and x-ray absorption²² measurements. Finally, looking at the extension into the GaAs buffer of the D profile recorded after the second, higher temperature annealing stage, we can confidently assert that the excess D is not bound to N. Moreover, it does not affect sizably the lattice or the electronic properties of GaAsN. It is worth noting here that no deuterium incorporation was measured, within experimental error, in several GaAs homoepitaxial layers deuterated following the same procedure used for GaAsN samples.

Data extracted from the deuterium concentration profiles giving the best fit to the $^2\text{H}(^3\text{He},p)^4\text{He}$ spectra are reported in Table II for two samples subjected to all the annealing stages. The second and the third columns give the deuterium doses measured in the GaAsN layer and in the GaAs buffer, respectively, the fourth column reports what percentage of the whole deuterium concentration (in GaAsN plus GaAs) is diffused into the GaAs buffer, and the last column gives the minimum (maximum) $[\text{D}]/[\text{N}]$ ratios computed by subtracting (or not) the concentration of the deuterium in excess measured at the interface from that measured in the GaAsN layer. Slight differences, evidenced in the table, were found for the temperatures of the two annealing stages, depending on the concentration and thickness of the samples. However, they do not affect the stoichiometry of the complexes. The data in Table II provide evidence that the excess D diffusing into the GaAs buffer is a small percentage of the total D in as-deuterated samples and at the end of the first annealing stage, whereas it becomes important after full dissolution of the passivating N-2D complex. The uncertainty in the excess D distribution profile justifies the width of the $[\text{D}]/[\text{N}]$ ratio interval reported in the last column. Finally, annealing up to complete dissolution of the complexes was performed on samples deuterated with different dose rates or by varying the cooling procedure at the end of the deuteration process (namely by keeping the sample for 10 min in deuterium atmosphere or by cooling it down immediately after D implantation). In all these cases, the $[\text{D}]/[\text{N}]$ ratio and its evolution do not depend on the dose rate and cooling procedure,

TABLE II. Deuterium doses as measured by $^2\text{H}(^3\text{He},p)^4\text{He}$ concentration depth profiles into the GaAsN layer (column 2) and into the GaAs buffer (column 3). Percentage of the total number of deuterium atoms which diffused into the GaAs buffer (column 4). The $[\text{D}]/[\text{N}]$ ratio is reported in column 5. This ratio was computed by considering all the deuterium into the GaAsN layer (max) or by subtracting from the whole deuterium into the layer a constant concentration value equal to the highest measured into the GaAs buffer (min).

Sample	d_{D} (10^{15} at./ cm^2) in GaAsN layer	d_{D} (10^{15} at./ cm^2) in GaAs buffer	% of D diffused	[D]/[N] ratio	
				min	max
E389 As D	22.77	2.57	10	2.5	3.5
E389+250 °C	13.71	2.14	13	1.6	2.2
E389+328 °C	3.01	4.10	60		0.5
E510 As D	11.05	1.95	15	2.3	3.4
E510+235 °C	8.57	1.75	17	1.9	2.7
E510+315 °C	0.81	0.98	55		0.3
E510+610 °C		0.27 ± 0.20			

whereas the amount of deuterium incorporated into the “excess” tail slightly depends on the cooling procedure.

IV. STRUCTURAL CHARACTERIZATION

In this section, we focus our attention on a more local investigation of N-D complexes and of their evolution with annealing. To this respect, XANES experiments at the nitrogen K edge revealed themselves as a powerful tool in determining the actual geometry of the N-H complex responsible for N passivation in GaAsN.²² Indeed, the best simulations of XANES line shapes of hydrogenated samples were unambiguously obtained by assuming the presence of a specific N-2H complex either in its symmetric or in its asymmetric configuration.²² The evolution of the XANES spectra with deuteration and annealings at different temperatures is shown in Fig. 5. In agreement with previous results, the shape of the absorption spectrum changes dramatically upon deuteration and is well simulated by assuming the formation of the N-2D complex.²² However, this shape is not affected sizably by the first low temperature (250 °C) annealing, while the pristine spectrum of the as-grown sample is completely recovered after the second annealing at high temperature (328 °C). This evolution supports the formation upon deuteration of a complex having a local structure around N (which is responsible for the XANES signature) not heavily modified with respect to the N-2D one, as it might be the case for a variant of the N-2D complex with a relatively weakly bound additional D atom.

Moreover, since the second annealing recovers the shape of the GaAsN spectrum, N atoms should go back to their substitutional sites and no deuterium atom still present in the samples should be bound to nitrogen.

This picture is confirmed definitely by ion channeling measurements, which have been performed contemporarily with RBS on the GaAs matrix and with NRA on deuterium and nitrogen signals.

Figure 6(a) shows the [001] axis channeling dips of the as-deuterated samples. We also show the GaAs dip of the

as-grown sample (triangles) in which nitrogen signal (not shown) is compatible with a complete substitutionality to the GaAs host matrix. The GaAs minimum yield, χ_{min} , and the width of the dip do not change before and after deuteration (stars), indicating that deuteration does not induce structural changes in the matrix. Channeling dips after deuteration suggest that nitrogen is displaced from regular lattice sites; in fact, no yield modification, with respect to the random signal, is measurable as a function of the tilt angle. Interestingly, the deuterium signal displays a low, but measurable, alignment with the host matrix. This could imply that nitrogen and deuterium in N-D complexes are slightly displaced toward the center of the channel but in a somehow ordered configuration. In other words, while the larger N atoms do not permit the probing beam to channel, smaller deuterium

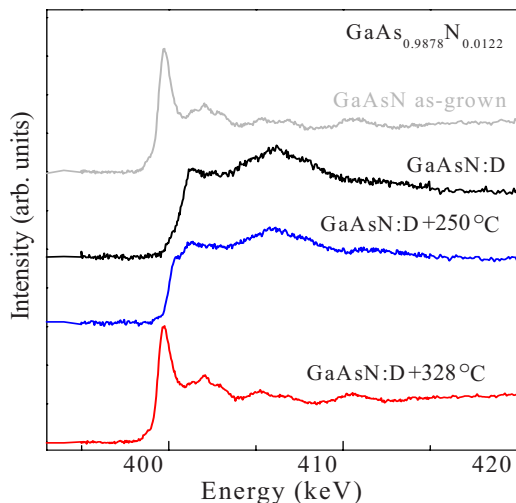


FIG. 5. (Color online) Nitrogen K -edge XANES spectra (fluorescence detection) of the same sample shown in the Figs. 2–4: as grown (first line from top), as deuterated with $d_{\text{D}}=3.0 \times 10^{18}$ cm^{-2} (second line from top), annealed at $T=250$ °C for 13 h (third line from top), and annealed at 328 °C for ~ 5 h (fourth line from top).

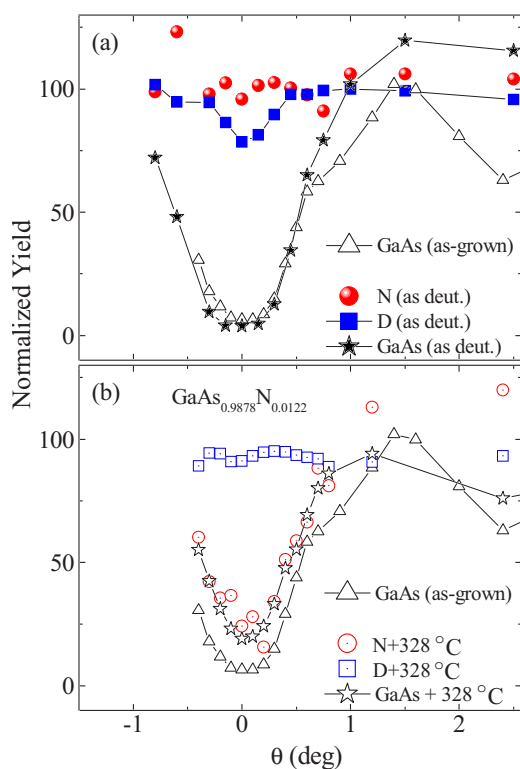


FIG. 6. (Color online) [001] axial channeling dips for GaAs (stars), N (circles), and D (squares), as measured with 1.2 MeV D^+ backscattering and $^2H(d,p)^3H$ and $^{14}N(d,\alpha)^{12}C$ reactions. (a) As-deuterated sample; (b) 328 °C annealed sample. Triangles correspond to the GaAs dip of the as-grown sample. Lines are drawn only to guide the eye.

atoms allow a small fraction of the beam to travel along the [100] direction.

The channeling dips do not change their shape after the first, low temperature annealing, whereas strong modifications are appreciable after the 328 °C annealing [Fig. 6(b)]. The tightening of the dip and the increment of χ_{\min} of the GaAs signal indicate that the structural quality of the GaAsN matrix has deteriorated, but the strongest modifications are displayed by both nitrogen and deuterium signals. In fact, the complete correspondence of the nitrogen signal to that of the matrix implies that nitrogen occupies substitutional sites again. On the contrary, the residual deuterium is now completely randomly located in the lattice, thus confirming that it is completely unrelated to both GaAs and N.

V. SUMMARY AND CONCLUSIONS

The whole set of structural and compositional characterizations reported so far allows a complete description of the process of N-D complex formation and dissolution. Deuterium reacts first with nitrogen and forms a passivating complex in which three D atoms are associated with a single N atom. In this complex, nitrogen and deuterium atoms are

displaced from substitutional GaAs lattice sites and the lattice parameter expands with respect to that of the GaAs buffer, thus giving rise to a compressive strain in the reacted layer. The deuteration process proceeds layer by layer, and the incorporation of further deuterium is possible only after the N-D complexes have been formed. Since it has been already demonstrated that the measured compressive strain depends solely on nitrogen concentration, while it is almost independent of hydrogenation conditions and of the N-hosting semiconductor matrix,¹⁵ we can argue that the N-3D complex is the final product of the deuteration in all dilute nitrides.

In agreement with previous suggestions based on HRXRD and PL measurements,¹⁵ only two different N-D complexes are responsible for the increase in the lattice parameter, which has been lost after thermal annealing at 250 °C and, of nitrogen passivation, which has been lost after thermal annealing at 328 °C. Upon the former moderate thermal annealing, the N-3D complex converts into a N-2D complex, still capable of N passivation, by losing one D atom which was bound to N less tightly than the other two atoms. This is indicated by the one unit change in the $[D]/[N]$ ratio determined by NRA, by the persistent passivation of N determined by PL, and XANES and channeling results. After an annealing at higher temperature (328 °C), N-2D dissolves, N atoms, previously displaced from the regular lattice sites, go back to their previous position, and the GaAsN lattice parameter and energy gap are almost fully recovered.

Some deuterium not bound to nitrogen is incorporated during (or at the end of) the deuteration process in a manner that depends slightly on deuteration conditions. This excess deuterium penetrates into the GaAs buffer layer and does not affect the band structure properties of GaAsN. Since this excess deuterium has not been observed upon deuteration of unstrained “defect-free” GaAs homoepitaxial layers, incorporation and diffusion of this extra D are most likely mediated by defects in the strained GaAsN:D layer and at the GaAsN-layer/buffer interface. The presence of deuterium not bound to nitrogen, and not detectable by PL, in the reacted layers might explain the controversial higher value of the H/N ratio (~ 5) recently reported in the literature.²⁴

Finally, a 600 °C annealing fully recovers the initial GaAsN lattice parameter and produces the total desorption of deuterium.

ACKNOWLEDGMENTS

M.B., G.B. and D.D.S. thank Camille Cohen and the Groupe de Physique des Solides of CNRS (Paris-France) for having supported some of the early NRA measurements. We acknowledge the strong encouragement by Antonio Drigo to investigate the structure of dilute nitrides by nuclear methods and his fundamental contribution in the early stage of this research.

*Corresponding author; berti@padova.infm.it

- ¹*Physics and Applications of Dilute Nitrides*, edited by I. A. Buyanova and W. M. Chen (Taylor & Francis, New York, 2004).
- ²*Dilute Nitride Semiconductors*, edited by M. Henini (Elsevier, Oxford, 2005).
- ³T. Taliercio, R. Intartaglia, B. Gil, P. Lefebvre, T. Bretagnon, U. Tisch, E. Finkman, J. Salzman, M.-A. Pinault, M. Lugt, and E. Tournie, *Phys. Rev. B* **69**, 073303 (2004).
- ⁴F. Masia, A. Polimeni, G. Baldassarri Hoeger von Hoegersthal, M. Bissiri, M. Capizzi, P. J. Klar, and W. Stoltz, *Appl. Phys. Lett.* **82**, 4474 (2003).
- ⁵G. Pettinari, A. Polimeni, F. Masia, R. Trotta, M. Felici, M. Capizzi, T. Niebling, W. Stolz, and P. J. Klar, *Phys. Rev. Lett.* **98**, 146402 (2007).
- ⁶A. Patane, A. Ignatov, D. Fowler, O. Makarovsky, L. Eaves, L. Geelhaar, and H. Riechert, *Phys. Rev. B* **72**, 033312 (2005).
- ⁷G. Pettinari, F. Masia, A. Polimeni, M. Felici, A. Frova, M. Capizzi, A. Lindsay, E. P. O'Reilly, P. J. Klar, W. Stolz, G. Bais, M. Piccin, S. Rubini, F. Martelli, and A. Franciosi, *Phys. Rev. B* **74**, 245202 (2006).
- ⁸G. Bisognin, D. De Salvador, C. Mattevi, M. Berti, A. V. Drigo, G. Ciatto, L. Grenouillet, P. Duvaut, and H. Mariette, *J. Appl. Phys.* **95**, 48 (2004).
- ⁹A. Polimeni, G. Baldassarri H. v., H. M. Bissiri, M. Capizzi, M. Fischer, M. Reinhardt, and A. Forchel, *Phys. Rev. B* **63**, 201304(R) (2001).
- ¹⁰G. Baldassarri H. von Hoegersthal, M. Bissiri, A. Polimeni, M. Capizzi, M. Fischer, M. Reinhardt, and A. Forchel, *Appl. Phys. Lett.* **78**, 3472 (2001).
- ¹¹A. Polimeni, M. Bissiri, M. Felici, M. Capizzi, I. A. Buyanova, W. M. Chen, H. P. Xin, and C. W. Tu, *Phys. Rev. B* **67**, 201303(R) (2003).
- ¹²A. Polimeni, G. Baldassarri Hoger von Hogersthal, F. Masia, A. Frova, M. Capizzi, S. Sanna, V. Fiorentini, P. J. Klar, and W. Stolz, *Phys. Rev. B* **69**, 041201(R) (2004).
- ¹³F. Masia, G. Pettinari, A. Polimeni, M. Felici, A. Miriametro, M. Capizzi, A. Lindsay, S. B. Healy, E. P. O'Reilly, A. Cristofoli, G. Bais, M. Piccin, S. Rubini, F. Martelli, A. Franciosi, P. J. Klar, K. Volz, and W. Stolz, *Phys. Rev. B* **73**, 073201 (2006).
- ¹⁴P. J. Klar, H. Gruning, M. Gungerich, W. Heimbrodt, J. Koch, T. Torunski, W. Stolz, A. Polimeni, and M. Capizzi, *Phys. Rev. B* **67**, 121206(R) (2003).
- ¹⁵G. Bisognin, D. De Salvador, A. V. Drigo, E. Napolitani, A. Sambo, M. Berti, A. Polimeni, M. Felici, M. Capizzi, M. Gungerich, P. J. Klar, G. Bais, F. Jabeen, M. Piccin, S. Rubini, F. Martelli, and A. Franciosi, *Appl. Phys. Lett.* **89**, 061904 (2006).
- ¹⁶A. Polimeni, G. Ciatto, L. Ortega, F. Jiang, F. Boscherini, F. Filippone, A. A. Bonapasta, M. Stavola, and M. Capizzi, *Phys. Rev. B* **68**, 085204 (2003).
- ¹⁷M. Felici, A. Polimeni, G. Salviati, L. Lazzarini, N. Armani, F. Masia, M. Capizzi, F. Martelli, M. Lazzarino, G. Bais, M. Piccin, S. Rubini, and A. Franciosi, *Adv. Mater. (Weinheim, Ger.)* **18**, 1993 (2006).
- ¹⁸A. Amore Bonapasta, F. Filippone, and P. Giannozzi, *Phys. Rev. B* **68**, 115202 (2003).
- ¹⁹M. H. Du, S. Limpijumngong, and S. B. Zhang, *Phys. Rev. B* **72**, 073202 (2005).
- ²⁰W. B. Fowler, K. R. Martin, K. Washer, and M. Stavola, *Phys. Rev. B* **72**, 035208 (2005).
- ²¹F. Jiang, M. Stavola, M. Capizzi, A. Polimeni, A. Amore Bonapasta, and F. Filippone, *Phys. Rev. B* **69**, 041309(R) (2004).
- ²²G. Ciatto, F. Boscherini, A. A. Bonapasta, F. Filippone, A. Polimeni, and M. Capizzi, *Phys. Rev. B* **71**, 201301(R) (2005).
- ²³A. Amore Bonapasta, F. Filippone, and G. Mattioli, *Phys. Rev. Lett.* **98**, 206403 (2007).
- ²⁴I. A. Buyanova, W. M. Chen, M. Izadifard, S. J. Pearton, C. Bihler, M. s. Brandt, Y. G. Hong, and C. W. Tu, *Appl. Phys. Lett.* **90**, 021920 (2007).
- ²⁵Hydrogen is a contaminant in most materials and introduces a source of systematic error in the measurements. Therefore, hydrogen has been substituted by its isotope deuterium in present experiments. Deuterium, which is negligibly present in the natural isotopic abundance, modifies electronic and structural properties of dilute nitrides as hydrogen does.
- ²⁶M. Berti, G. Bisognin, D. De Salvador, E. Napolitani, in *Contents of Recent Books in Physical Sciences*, edited by G. Salviati, T. Sekiguchi, and A. Gustafsson (Research Signpost, Kerala, India, in press).
- ²⁷W. Moller and F. Besembacher, *Nucl. Instrum. Methods* **168**, 111 (1980).
- ²⁸H. S. Bosch and G. M. Hale, *Nucl. Fusion* **32**, 611 (1992).
- ²⁹D. Dieumegard, D. Dubreuil, and G. Amsel, *Nucl. Instrum. Methods* **166**, 431 (1979).
- ³⁰*Handbook of Modern Ion Beam Materials Analysis*, edited by J. R. Tesmer and M. Nastasi (Materials Research Society, Pittsburgh, 1995).
- ³¹M. Mayer, SIMNRA user/s guide, <http://www.rzg.mpg.de/mam/MANUAL.pdf>
- ³²L. Floreano, G. Naletto, D. Cvetko, R. Gotter, M. Malvezzi, L. Marassi, A. Morgante, A. Santaniello, A. Verdini, F. Tommasini, and G. Tondello, *Rev. Sci. Instrum.* **70**, 3855 (1999).